Sol-Gel Synthesis of Titanium/Bismuth Oxide Coatings for Biocompatibility Applications on 316L Stainless Steel

Jorge Bautista-Ruiz[1*], Willian Aperador[2] and J. C. Caicedo[3]

[1]Department of Electromechanical Engineering, Universidad Francisco de Paula Santander, San José de Cúcuta, Colombia; jorgebautista@ufps.edu.co
[2]Universidad ECCI, Bogotá, Colombia; jbautistaruiz@yahoo.es
[3]Tribology Polymers, Powder Metallurgy and Processing of Solid Recycled Research Group, Universidad del Valle, Colombia; jcaicedoangulo1@gmail.com

Abstract

Objectives: This study was carried out in order to establish the potential offered by the sol-gel method to obtain Titanium/Bismuth oxide coatings on 316L Stainless Steel (SS) substrates in biocompatibility applications. Methods/Analysis: The stable sol was synthesized by using Bismuth nitrate (III) pentahydrate and Titanium (IV) butoxide. The coatings were deposited by spin-coating technique at 4000 rpm and characterized topographically by Scanning Electron Microscopy SEM and structurally by X-ray diffraction XRD. Through the techniques of polarization potentiodynamic curves and Electrochemical Impedance Spectroscopy (EIS), the anticorrosive response of the films was evaluated. The thickness was then measured, and biocompatibility test was developed. Findings: It was found that the coatings with high composition of the precursor titanium (IV) butoxide offer the best results as an anticorrosive application. Likewise, the growth of cells was uniform on the films indicating that the medium offered by the films does not present active cytotoxicity and surpasses by a large number the cellular growth level compared to stainless steel. Applications /Improvement: 316L (SS) is very useful in implantology, for its low cost compared with other materials. The implanted steel suffers corrosion by the physiological fluids of body. Titanium/Bismuth coatings establish a barrier between body fluids and SS implant.

Keywords: Biocompatibility, Corrosion, Sol-gel, Titanium/Bismuth Oxide Coatings, 316L

1. Introduction

The sol-gel method is a process of synthesis of materials currently of great interest[1]. The term sol–gel refers to a process in which solid particles dispersed in a liquid (sol, mostly colloidal) agglomerate together to form a continuous three-dimensional (3D) network extending throughout the liquid (gel)[2,3]. This procedure consists of three main parts: a) the preparation of the sol, b) gelation of the same, and c) removing the solvents[1]. Sols can be made from inorganic salts or molecular precursors known as metal alkoxides. In the system, they form a molecular network due to condensation reactions of mainly hydrolysed, and the microstructure, which is strongly formed depending on the experimental conditions. Molecular precursor

hydrolysis and reaction with water are usually performed in the presence of an acidic or basic catalyst, which allows control of the rate and extent of the hydrolysis reaction[1]. This method of preparation of materials has been applied in various fields of materials science. The fields range from inorganic materials to organic and biological systems, surfaces with superhydrophobic and super-oleophobic characteristics[4], the development of biosensors for medical diagnosis[5], fuel cells[6,7], superconductors[8,9], ceramic composites[10] and dental ceramics[11], and other materials of varied composition.

Since sol–gel processes can occur under extraordinarily mild thermal conditions, and due to the unique combinations of properties and numerous inherent advantages such as better homogeneity and purity,

easier controllability of size and shape, and enhanced manageability, sol–gel technology has found ever-increasing applications in a diverse range of scientific and engineering fields[3,12].

In the present study, a composite Bismuth-Titanium oxide coating was synthesized via sol-gel method at room temperature. These stable soles were formed in molar concentrations [Ti/Bi: 20/80], [Ti/Bi: 50/50] and [Ti/Bi: 80/20] using as precursors Titanium (IV) butoxide $Ti(OBu)_4$ and Bismuth nitrate (III) pentahydrate $(Bi(NO_3)_3 \cdot 5H_2O)$, 2-Ethoxyethanol $(C_4H_{10}O_2)$ and acetic acid $(C_2H_4O_2)$ as solvents, and Ethanolamine C_2H_7NO as complexing. A commercial AISI 316L austenitic stainless is used in this work as substrate. The coatings were deposited at 4000 rpm by spin-coating tecnique. Additionally, the films were characterized topographically by Scaning Electron Microscopy SEM, X-ray diffraction XRD, the thickness was measured, and biocompatibility test was developed. Anticorrosive response was evaluated in a simulated physiological solution, Ringer's solution, using Potentiodynamic Curves and of Electrochemical Impedance Spectroscopy - EIS techniques. It was found that the coatings with high composition of the precursor titanium (IV) butoxide offer the best results as an anticorrosive application as well as the evolution of cells is homogeneous on films indicating that the medium offered by the films does not present active cytotoxicity and surpasses by a large number the cellular growth level compared to stainless steel. This study allowed establishing the potential offered by coatings in applications of biocompatibility.

2. Sample Preparation and Experimental Techniques

2.1 Materials

The chemical reagents used were: as precursors bismuth nitrate (III) pentahydrate - $Bi(NO_3)_3 \cdot 5H_2O$ (Alfa Aesar, 98%) and Titanium (IV) butoxide - $Ti(OBu)_4$ (Aldrich, 98%); as solvents glacial acetic acid (Aldrich, 99.7 +%) and 2-ethoxyethanol (Aldrich, 99%), and ethanolamine (Aldrich, 98%) as complexing agent.

2.2 Bismuth-Titanium Oxide Composite

The solution (sol) of bismuth-titanium oxides was prepared by modifying the method established by[13,14].

Sol synthesis was sintetized in two solutions, A and B. In solution A, 10g of Bi (NO_3) were dissolved in 25 ml of acetic acid while stirring for 2 hours at room temperature. Solution B contained Titanium (IV) butoxide to the molar concentration [Ti/Bi: 20/80], [Ti/Bi: 50/50] and [Ti/Bi: 80/20], at room temperature for 2 hours in constant stirring. Then, solutions A and B were mixed keeping the agitation for 3 hours. Finally, the ethanolamine was added until a pH = 4 were reached to avoid hydrolysis of the bismuth ions. To decrease the amount of water in the final compound, Bi $(NO_3)_3$ $5H_2O$ was dried under vacuum at 70 °C for 96 hours. Figure 1 shows the general scheme of synthesis.
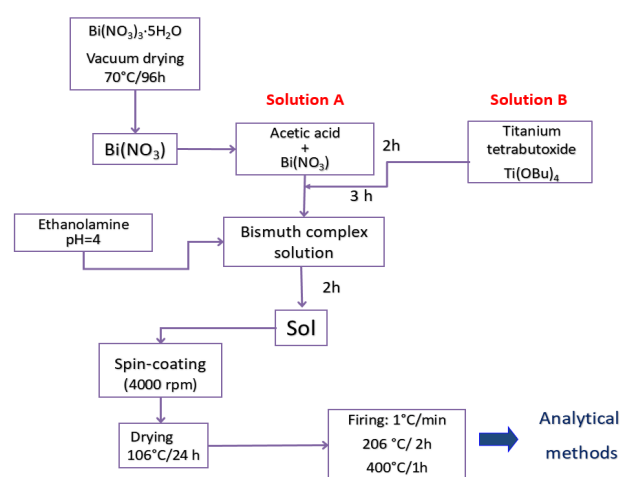

Figure 1. Titanium/Bismuth oxide synthesis sol.

In this investigation, the molar concentrations of the precursors of bismuth and titanium, and the amount of precursor by concentration are related in Table 1.

Table 1. Amount of reagents for Titanium/Bismuth oxides

Sample	$Bi(NO_3)_3$ (g)	$Ti(OBu)_4$ (ml)	$C_2H_4O_2$ (ml)
[Ti/Bi: 20/80]	18.16	25.22	
[Ti/Bi: 50/50]	26.12	9.08	50
[Ti/Bi: 80/20]	28.54	2.54	

2.3 Titanium/Bismuth Oxide Coatings

Substrates made of stainless steel 316 L (SS) with dimensions of 3.5 cm x 2.5 cm x 0.32 cm, were polished with silicon carbide papers numbers 80, 120, 160, 220,

240, 360, 500, 1000 and 1200, and alumina. Subsequently, residual oil, dust and residual metals were removed with acetone in an ultrasonic bath for 10 minutes. Then, they are dried with hot air for 3 minutes. The films are formed at room temperature, using the spin-coating technique at 4000 rpm and for 10 s.

The coatings were formed with sols of 900 hours of aging. Subsequently, they were dried in an oven at 106 ° C for 24 hours. The films are sintered at a heating rate of 1 ° C / min up to 206 ° C stabilizing for 2 hours at this temperature. It is then brought to 400 ° C at the same initial heating rate and stabilized for one hour. Finally, they cool down, Figure 1.

2.4 Characterization

The electrochemical impedance spectroscopy tests were developed in a three-electrode cell: Ag/AgCl reference electrode; platinum electrode as counter electrode; working electrode substrate-coating system with an exposure area of 1 cm^2. The test solution was Ringer´s solution at 37 °C. Frequency ranges from 0.01 Hz to 100 kHz. Scanning potential of 10 mV. The EIS data were analysed by fit to a proposed equivalent electric circuit model and constituted by capacitances and resistances, with the Gamry Echem Analyst software with the nonlinear method of least squares method based on iterations.

The Tafel polarization assays were carried out in a three-electrode cell: 1) Ag/AgCl reference electrode, 2) platinum as counter-electrode and 3) sample as electrode work. The analysis area was 1 cm^2, the scanning was 1 mV/s in Ringer´s solution. The range of potential that was swept was from -200 mV to 200 mV with respect to the corrosion potential (Ecorr). Speeds and corrosion potentials were obtained by extrapolation of Tafel using a GAMRY Instruments potentiostat-galvanostat 3000. The study was carried out using the Echem Analyst program. The equipment has a voltage resolution of 20 V and current of 1fA; this resolution is sufficient for the tests to be performed. The immersion time before the test was 45 minutes. For each coating three potentiodynamic tests were performed.

Corrosion current density (i_{corr}) and Corrosion potential (E_{corr}) values are determined by the Tafel extrapolation method using the Gamry Echem Analyst software 5.3.

In the characterization of the surface morphology and its elemental composition, a scanning electron microscope (COXEM-CX200TM) and X-ray spectral analyzer (Z1 Ametek) were used. In the microprobe analysis, the composition of the elemental was determined by the average of 5 areas of 300 x 200 μm^2 randomly selected. The depth of the analysis was up to 5 μm.

In the determination of the crystalline parameters, a Panalitycal-Empyream diffractometer was used in Bragg-Brentano geometric configuration, copper K$_\alpha$ line (1.540998 Å), current strength of 30 mA, potential difference of 40 kV, sweep of 20° to 90° (2θ), step time of 0.50 s and step size of 0.020° (2θ) in continuous mode.

The measurement of thicknesses, a DEKTAK 150 profilometer with 6 Å repeatability, valley and ridge profile, 600 μm scan, 30 s time, 1 mg force and 0.067 μm resolution / sample was used.

2.5 Biocompatibility

Cell adhesion: For the cell adhesion process the samples of the coatings were used as well as for the substrate AISI 316 L SS. For assay, cells were incubated for 24 hours in 500 μl of culture medium under standard conditions, as described above. After incubation, cells without adhering to the substrate were removed through four washes with sterile water. Cells that remained attached to the substrate were fixed and stained with 300 μl of a solution composed of 0.1% toluidine blue and 3.5% paraformaldehyde. After 24 hours at room temperature, 100 μl of the supernatant was used to measure the optical absorption at 630 nm by an enzyme-linked immunosorbent assay. The objective is to determine the absorbance related to the number of cells adhered to the substrate.

Cellular Proliferation: The assay determines the capability of the mitochondrial succinate dehydrogenase enzyme for the metabolic reduction of 3-(4, 5-dimethylthiazol-2- Yl) -2, 5-diphenyltetrazole (MTT). This reduction results in a blue colored compound (formazan) which determines the cellular mitochondrial performance. This method allows establishing cell proliferation, taking into account the proportional relationship between living cells and the amount of formazan produced.

The cells were seeded and incubated in periods of 24, 48, 120, 144 and 168 hours. To the cultures, 500 μl of fresh medium and antibodies were added daily. At the end of each period measured in hours, the cells were incubated

for an additional 4 hours by adding 60 μl of MTT at 37 ° C. Subsequently, the supernatant was removed and 250 μl of dimethyl sulfoxide (DMSO) was added to each cell culture. At 30 minutes of incubation the absorbance at 570 nm was measured.

3. Results and Discussion

3.1 Electrochemical Impedance Spectroscopy – EIS

Figure 2 shows the Nyquist diagrams for the coatings obtained from stable sols of the Bismuth-Titanium oxide system at concentrations [Ti/Bi: 20/80], [Ti/Bi: 50/50] and [Ti/Bi: 80/20] with 4000 rpm spin speed. The electrolyte used was Ringer's solution, which simulates the conditions of the body fluids.
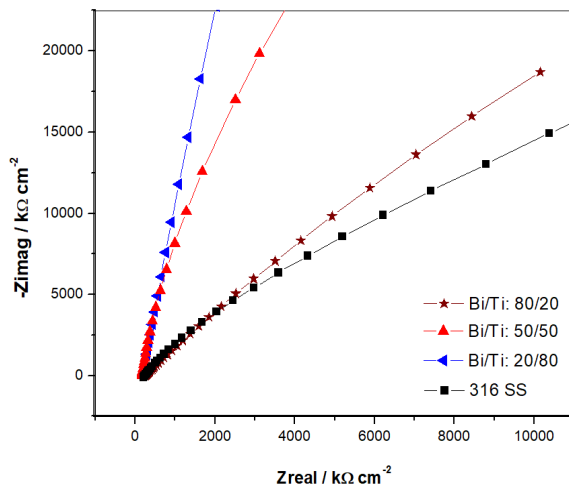

Figure 2. Comparison of Nyquist graphs of Titanium/Bismuth Oxide coatings.

The EIS analysis focuses mainly on the polarization resistance values, Rp. This is the resistance that the coating opposes the passage of ions from the solution to the substrate, preventing it from corroding. In general terms when a coating registers a high value of resistance to the polarization it will be possible to conclude that it is a good anticorrosive protector.

Figure 2 shows the same behaviour of the Nyquist diagrams, that is, all the graphs are open. This behaviour, shows high values of resistance to polarization and, therefore, low corrosion rates. An open shape, greater than that for the substrate, is observed. This shows that the films deposited on the substrate 316L act as a protective barrier

Table 2. Equivalent circuit parameter values for Titanium/Bismuth oxide coatings

Sample	$Rsol$ (Ωcm^2)	Rpo (Ωcm^2)	Rco (Ωcm^2)	$Ccor$ $(\mu F\ cm^{-2})$	Cc $(\mu F\ cm^{-2})$
[Ti/Bi: 80/20]	225.8	419.6x10³	236.8	2954x10⁻¹²	7.08x10⁻⁹
[Ti/Bi: 50/50]	244.8	921.6x10³	585.0	1481x10⁻⁶	54.5x10⁻⁹
[Ti/Bi: 20/80]	254.3	250.0x10³	138.6	672x10⁻³	66.7x10⁻⁶

when in contact with the Ringer's solution. These results and their correlation with the values of resistance to polarization recorded in Table 2. This shows a direct relationship between the anticorrosive effectiveness of the films and the corresponding concentration of titanium precursor.

The comportments described in Figure 2 are modelled with the equivalent circuit of Figure 3. This equivalent circuit relates to a metal substrate coated with layers of ceramic material. The result is showed with those corresponding to the obtained between the coating and the substrate and its chemical-mechanical interaction. The bismuth/titanium oxide coating is analysed as a single element, so that an alternating current scheme is corresponding to the equivalent circuit where there is a resistance to polarization that indicates the performance of the protective layer in parallel with a constant phase element, evidencing the adequate adherence of the coating to 316L substrate (Figure 3)[15].

The values of each parameter or constituent elements of the equivalent circuit for each of the coatings studied are recorded in Table 2. From the information given in these tables an average value is established for the resistance to the working solution, in this case Ringer's solution, 220.59 Ω.
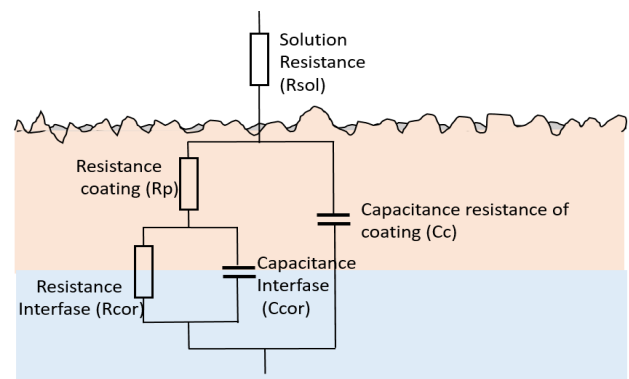

Figure 3. Equivalent electrical circuit.

To complement this study, the percentage of porosity of the Bismuth/ Titanium oxide coatings system is estimated by equation[16–19].

$$Pf_{Rp} = \frac{R_{p,u}}{R_{p,r-u}} \qquad (1)$$

where, Pf_{Rp} is the percent porosity of the coating in terms of polarization resistance, $R_{p,u}$ and the polarization resistance of the film? $R_{p,r-u}$

The percent porosity values are recorded in Table 3. According to the information it is observed that the percentage of porosity for all Titanium/Bismuth oxide coatings system is very low, so much that it is not reached to 0.1%. These results allow inferring the conformation of homogeneous films free of cracking and porosity, as corroborated by SEM analyses.

Table 3. Porosity factor values for Titanium/Bismuth oxide coatings

Sample	Pf_{Rp} (%)
[Ti/Bi: 80/20]	1.4
[Ti/Bi: 50/50]	0.8
[Ti/Bi: 20/80]	0.2

3.2 Potentiodynamic Polarization Curves

The graphs of Figure 4 reveal the Tafel polarization diagrams of Bismuth-Titanium oxide coatings for the molar concentrations [Ti/Bi: 20/80], [Ti/Bi: 50/50] and [Ti/Bi: 80/20], and its comparison with respect 316L substrate. The variation of corrosion potentials of the coatings with respect to the corrosion potential of the substrate is observed. It can be seen that all the curves are above the one corresponding to AISI 316L (SS) indicating corrosion potential more positive and therefore that there is a less tendency to suffer corrosion in saline medium, it is also observed that these curves are shifted to the left
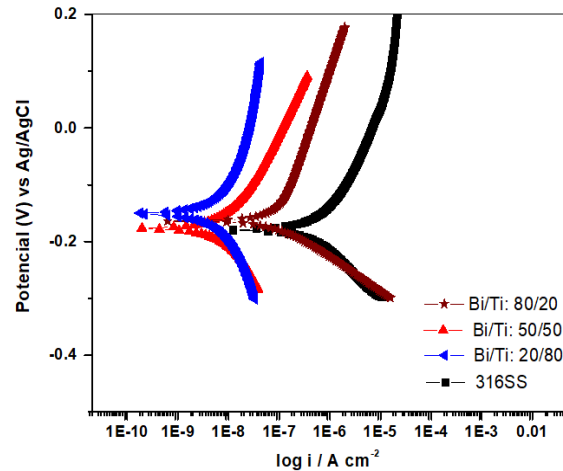

Figure 4. Polarization potentiodynamic curves of Titanium/Bismuth Oxide coatings and the substrate 316L.

which allows to infer that the current density of corrosion is lower in the coatings with respect to 316L (SS) substrate. It is important to note that concentrations have a better anticorrosive performance than others; this is concluded when comparing the results of corrosion potential values and corrosion current for the concentrations studied, as shown in Table 4. To know the trend of the parameters mentioned above will allow knowing the behaviour of the substrate-coating interface in each case.

One way to evaluate the corrosion resistance of coatings is through their corrosion current density and their corrosion potential, the most resistant films would be those that conjugate a low corrosion current (icor) with corrosion potential Ecorr noble.

According to the results obtained, it can be concluded that the corrosion potentials recorded for the films, without concentration discrimination, are more positive in comparison to Ecorr of 316L SS substrate. The results of the study show that coatings [Ti/Bi: 80/20] present more noble corrosion potentials.

In terms of corrosion rates, it is observed that low amounts of the bismuth precursor lead to films with

Table 4. Values of the parameters according to the Tafel polarization curves

Sample	β anodic (mV/decade)	β cathodic (mV/decade)	Icorr (nA)	Ecorr (mV vs Ag/AgCl)	Corrosion rate (mpy)
[Ti/Bi: 80/20]	6.910 x10^{-3}	1.824	15.05	-159.0	6.89 x10^{-3}
[Ti/Bi: 50/50]	201.1 x10^{-3}	236.8 x10^{-3}	16.10	-182.0	7.05 x10^{-3}
[Ti/Bi: 20/80]	342.9 x10^{-3}	67.70 x10^{-3}	137.0	-164.0	62.34 x10^{-3}
316L (SS)	586.95	224.9	840.70	-180.0	880.80 x10^{-3}

high corrosion rates. Correlating with the SEM results, on these coatings tend to the formation of more bismuth oxides in the sintering process.

It is also possible to determine the percentage of protective effectiveness $Ef(\%)$ of Bismuth-Titanium oxide coatings varying the concentration of precursors and spin speeds, as[16–19]:

$$Ef(\%) = \left(\frac{I_{corr_s} - I_{corr_f}}{I_{corr_s}} \right) \times 100 \qquad (2)$$

where, I_{corr_s} is the corrosion current density of the uncoated substrate and I_{corr_f} is the corrosion current density of the coated substrate.

Table 5 shows the values for the percentage of protective effectiveness. From the calculations it is identified that [Ti/Bi: 80/20] and [Ti/Bi: 50/50] films provide a percentage of protective effectiveness greater than 95%. The lowest percentage of anti-corrosive effectiveness is presented by [Ti/Bi: 20/80] coatings, due to proliferation of Bismuth oxides and Titanium oxides that lead to the appearance of micro-pores, allowing some Ions of the Ringer's solution reach the substrate.

Table 5. Protective factor effectiveness values for coatings

Sample	Pf_{Rp} (%)
[Ti/Bi: 80/20]	98.52
[Ti/Bi: 50/50]	98.47
[Ti/Bi: 20/80]	85.60

3.3 Thickness

Final thickness of the film is influenced by the growth of the Bismuth oxides and Titanium oxides, as evidenced by SEM micrographs. It was found that high contents in the Bismuth precursor allow obtaining thinner coatings. Table 6 shows the values for the thickness.

Table 6. Thickness values

Sample	Thickness (nm)
[Ti/Bi: 80/20]	155.84
[Ti/Bi: 50/50]	108.06
[Ti/Bi: 20/80]	93.48

3.4 Scanning Electron Microscopy (SEM)

Figures 5–7 shows the results obtained by SEM technique of the Bismuth-Titanium oxides coatings as a function of the precursor's concentration.

Figure 5 a) presents the morphology, at 1000X, of a coating in composition [Ti/Bi: 20/80], a homogeneous surface free of cracks or pores is evident. Figure 5 b) shows the corresponding elemental chemical analysis, indicating elements such as Ti, Bi and O, corresponding to the film. Also, elements such as: Cr, Fe and Ni components of the substrate 316L-SS are manifested.

Figure 6 a), shows the surface characteristics of [Ti/Bi: 50/50] coatings at a spin speed of 4000 rpm. It shows a homogeneous topography with very little growth of Bi-Ti oxides. The surface irregularities are not so noticeable
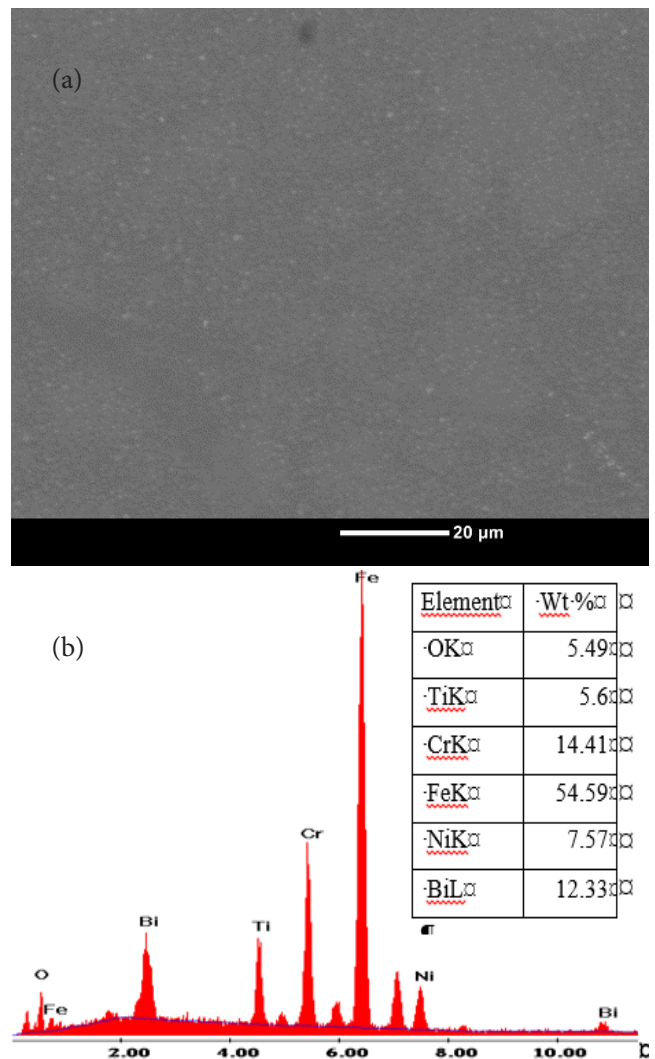

Element	Wt-%	
OK	5.49	
TiK	5.6	
CrK	14.41	
FeK	54.59	
NiK	7.57	
BiL	12.33	

Figure 5. [Ti/Bi: 80/20] coating, a) SEM micrograph at 1000x b) Elemental compositional analysis.

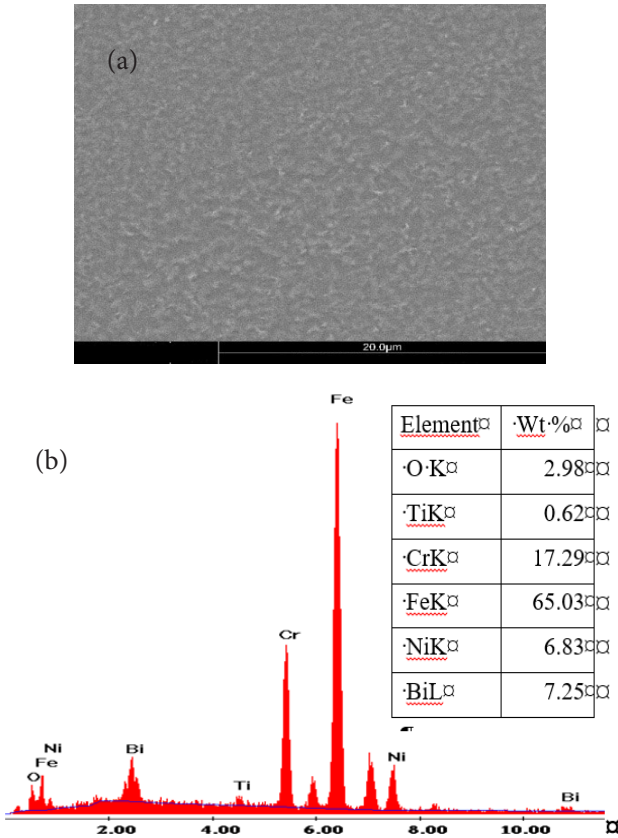| Element	·Wt·%¤	¤
·O·K¤	2.98¤¤	
·TiK¤	0.62¤¤	
·CrK¤	17.29¤¤	
·FeK¤	65.03¤¤	
·NiK¤	6.83¤¤	
·BiL¤	7.25¤¤	

Figure 6. [Ti/Bi: 50/50] coating, a) SEM micrograph at 4000x b) Elemental compositional analysis.

which leads to a surface with little roughness. In Figure 6 b), it shows the elemental chemical spectrum, both in the substrate and in the coating, due to the thin film thickness. It is evident that the ceramic film is formed by elements such as Bi and Ti. The other elements such as Fe, Ni and Cr refer to the proper composition of the substrate 316L.

The surface characterization of [Ti/Bi: 20/80] coating is presented in Figure 7. In general, it is observed that in the films no bismuth oxides are formed in the form of grain, as described for the other coatings of the Ti/Bi system. It is evidenced the growth of ramifications, proper behaviour of bismuth salts. In Figure 7a, emphasis is placed on the characterization of the observed branching. The elemental chemical analysis of the branch shows that its composition is related to the growth of oxides of the elements Bi and Ti. Elements such as Fe, Ni and Cr are typical of the substrate.

3.5 X-Ray Diffraction (XRD)

Figure 8 shows the results by XRD technique to Bismuth-Titanium oxide coatings. It was observed that none of the
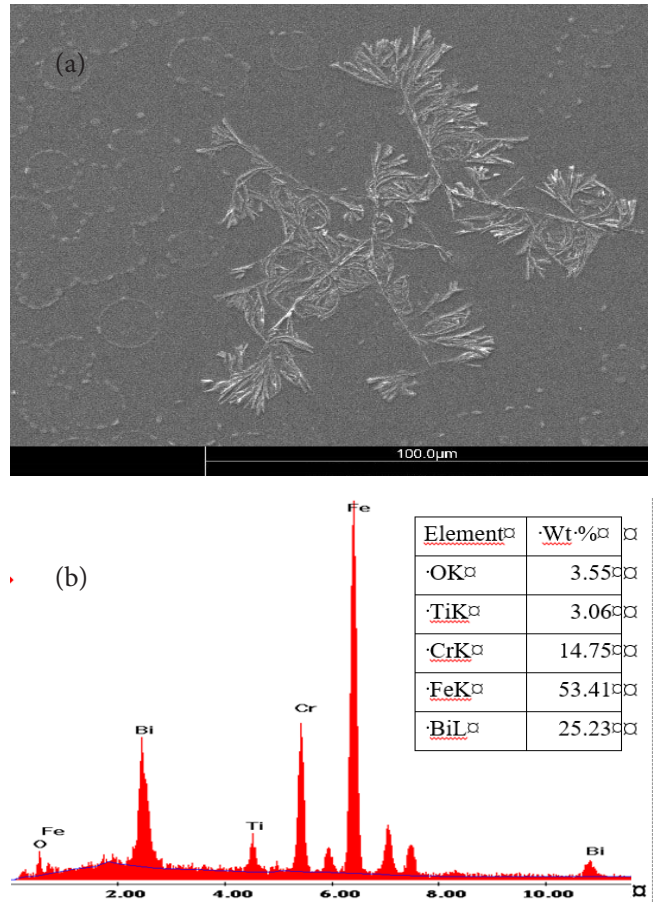

Element	·Wt·%¤	¤
·OK¤	3.55¤¤	
·TiK¤	3.06¤¤	
·CrK¤	14.75¤¤	
·FeK¤	53.41¤¤	
·BiL¤	25.23¤¤	

Figure 7. [Ti/Bi: 20/80] coating, a) SEM micrograph at 1000x b) Elemental compositional analysis (branch).
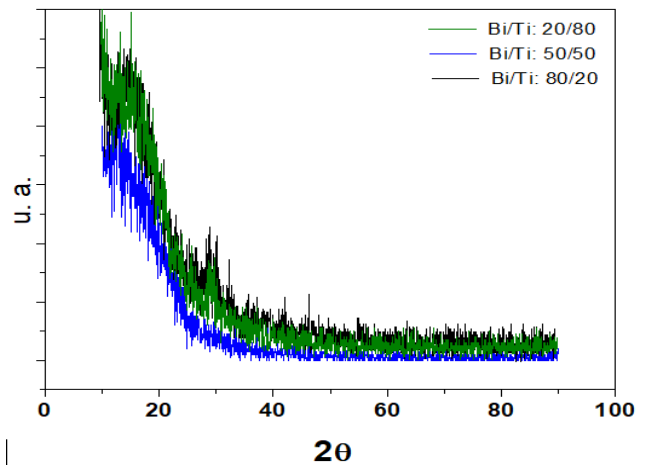

Figure 8. Diffractogram of Titanium/Bismuth oxides coatings.

films evidenced a crystalline structure due, quite possibly, to the sintering temperatures used in the consolidation

process of the films, which were not sufficient to crystallize the compound, as suggested by[20].

3.6 Biocompatibility

3.6.1 Cell Adhesion Assay

In Figure 9, the results of osteoblast adhesion are presented depending on the type of coating and the 316L (SS) substrate. It was found that the best results are related to coatings with higher content of titanium, which allows to establish a directly proportional relation between high concentrations of the precursor of the titanium and greater number of cells adhered to coating. In the investigation it was found that [Ti/Bi: 80/20] films show the best results of cell adhesion, and type [Ti/Bi: 20/80] coatings have the lowest efficiency in terms of cell adhesion. Based on these results of cell adhesion of osteoblast cells, it was established that all coatings establish optimal cell growth conditions; otherwise it happens with uncoated 316L substrate. The reliability levels for the results were 80% established from the 24 hours of incubation.
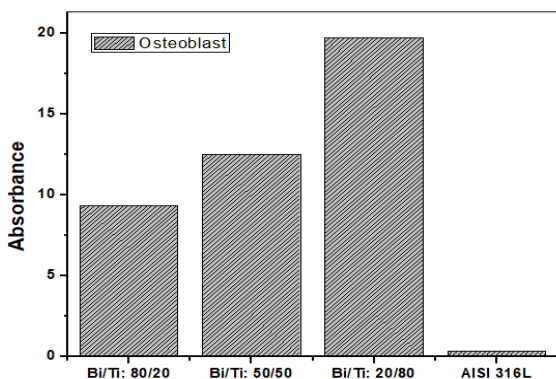
Figure 9. Absorbance results for osteoblast cells.

3.6.2 Cytotoxicity and Cell Proliferation with MTT Assay

The objective of the test was to determine the potential cytotoxic effects of coatings on cell cultures. The assay is based on the metabolic reduction of 3 (4, 5-dimethyl-2-thiazoyl) -2,5-diphenyltetrazole (MTT) bromide to its insoluble form. This process is developed by the mitochondrial enzyme succinate dehydrogenase in relation to the mitochondrial function of osteoblast cells. In this assay, the quantity of formazan is related as an indicator of viability, Figure 10. As the formazan crystals are retained by the cell by dissolution in isopropanol and
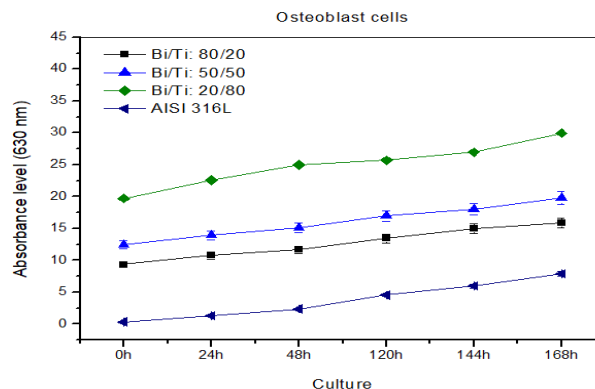
Figure 10. Osteoblast cell proliferation.

by measuring its absorbance, the amount generated in the process is quantified.

According to the cytotoxicity results obtained for the coatings, it can be deduced that films [Ti/Bi: 80/20] have the highest absorbance values, 20.90. For the films [Ti/Bi: 50/50], the absorbance reaches values of 14.30. With respect to films [Ti/Bi: 20/80] the absorbance value reaches 11.50. All measurements were taken at 168 hours of cell incubation. The study shows that regardless of the amount of the Ti precursor component of the films, the absorbance values are higher with respect to the information obtained from the cells anchored in the uncoated substrates. The graph of Figure 10 shows the cell proliferation of the osteoblasts deposited on the coatings. The study also showed that films offer a beneficial bioactive medium represented in homogenous cell growth.

Figure 11 shows the graphs in which the number of osteoblast cells is related to the incubation time. It is observed that the absorbance and cell growth values are directly proportional. According to the results, the coating [Ti/Bi: 80/20] establishes the largest number of cells. Minimum cell values are recorded for coatings [Ti/Bi: 20/80]. These results are related to the concentrations of the Bismuth precursor. The greater the amount of Bi that make up the coating, the effectiveness of the cell support medium decreases. From the study it was concluded that the combinations of Bi or Ti precursors that make up the films are indifferent because all the coatings offer an adequate medium for cell growth. Specifically, the coating with the highest concentration of the titanium precursor favours the proliferation of osteoblasts cells.

The adhesion of the cells to the coatings is related by the dissipation of energy of the osteoblasts in the incubation time. The structuring of proteins such as fibronectin, vitronectin and fibrogen in the extracellular
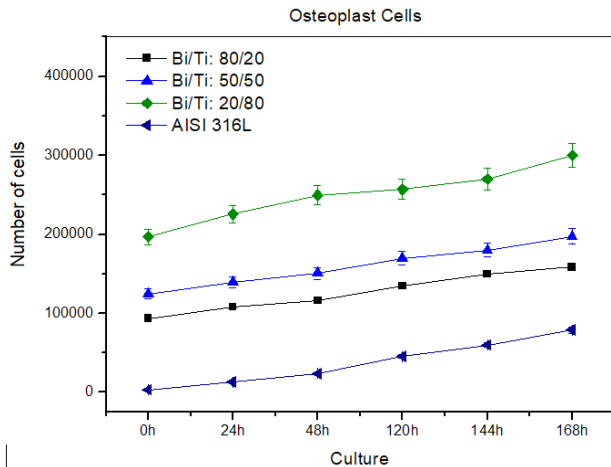
Figure 11. Cell proliferation of osteoblasts as a function of incubation time.

matrix, favour the adhesion of the cells to the surface of the films and the substrate 316L (SS). The results of the investigation showed that the adhesion of osteoblasts is greater in coatings with high concentrations of the titanium precursor, due to the martensitic and equiaxial α microstructure of titanium which favours the replication of fibronectin and fibrogen.

Cytotoxicity assays allow to establish the toxic potential of the material in the cells. It is necessary that the cells adhere to the surface of the coatings and evaluate if the medium is optimal to grow, proliferate and develop their normal metabolic functions. During the incubation time of the osteoblasts the free radicals released were minimal observed behaviour because they did not affect cell reproduction and metabolic processes.

When comparing the absorbance curves and the number of cells adhered to the coatings (Figure 9 and Figure 10), an adequate metabolic performance of the osteoblasts is observed in the incubation time. The cell adhesion process is carried out by means of proteins present on the surface of the coatings and the protein, integrin, of the cell membrane. The interaction between the integrin and the extracellular proteins in the coating establishes the processes of cell proliferation.

The coating composed of Ti is exposed to the contact of blood cells, a titanium complex is formed spontaneously indicating that titanium reacts with water, mineral ions and plasma fluids and that the Low pH of the implant bed, accelerates the formation of calcium phosphate on the surface material. The oxide surface must be considered as a dynamic, non-passive system. The oxide surface plays an important role in the remodelling process that creates an adaptive interface, rather than a simple boundary between the material and the cells, so that the reactive nature of this oxide, with its spontaneous formation of calcium-phosphate-apatite, is what makes titanium biocompatible.

It is also important to emphasize that the biological response to Titanium oxide is dynamic and changing. One method to evaluate the biological response is through cell adhesion because the cell generation and absorbance levels reveal the applied charge and generating a process of progressive altering by means of the bond between the biomolecules and the determined surface by the adsorption occurred.

4. Conclusions

The anticorrosive effectiveness of the coatings is proportional to the amount of Titanium precursor that forms the films, which is corroborated by the SEM analysis, establishing surfaces with good homogeneity, good sealing and free of micropores or microcracks. High concentrations of the Bi precursor that make up the films, allow obtaining thinner coatings.

It was observed that none of the films evidenced a crystalline structure due, quite possibly, to the sintering temperatures employed in the process of consolidating the films, which were not sufficient to crystallize the compound.

Cell adhesion, cytotoxicity and cell proliferation assays have allowed to evaluate the adhesion of osteoblasts on the surfaces of the coatings and substrate. During the incubation time of the osteoblasts, the free radicals released during the cell incubation time did not affect the metabolic processes and cellular reproduction. From the study it was concluded that the combinations of Bi or Ti precursors that make up the films are indifferent because all the coatings offer an adequate medium for cell growth. Specifically, the coating with the highest concentration of the titanium precursor favours the proliferation of osteoblasts cells.

5. Acknowledgement

OBTENIDOS VÍA SOL-GEL SOBRE ACERO 316L, announcement 032/2018.

6. References

1. Bautista-Ruiz J, Aperador W, Delgado A, Díaz-Lagos M. Synthesis and characterization of anticorrosive coatings of SiO2-TiO2-ZrO2 obtained from sol-gel suspensions. International Journal of Electrochemical Science. 2014 May; 9:4144–57.

2. Brinker C, Scherer G. Sol–gel science: The physics and chemistry of sol–gel processing. San Diego: Academic Press; 1990.

3. Amiri A. Solid-phase microextraction-based sol–gel technique. TrAC Trends in Analytical Chemistry. 2016; 75:57–74. Crossref

4. Wu X, Fu Q, Kumar D. Mechanically robust superhydrophobic and super-oleophobic coatings derived by sol–gel method. Materials and Design. 2016; 89:1302–9. Crossref

5. Oubaha M, Gorin A, McDonagh C, Duffy B. Development of a multianalyte optical sol–gel biosensor for medical diagnostic. Sensors and Actuators B: Chemical. 2015; 221:96–103. Crossref

6. Cao X, Jiang S, Li Y. Synthesis and characterization of calcium and iron co-doped lanthanum silicate oxyapatites by sol–gel process for solid oxide fuel cells. Journal of Power Sources. 2015; 293:806–814. Crossref

7. Setsoafiaa D, Hinga P, Junga S. Sol–gel synthesis and characterization of Zn2+ and Mg2+ doped La10Si6O27 electrolytes for solid oxide fuel cells. Solid State Sciences. 2015; 48:163–70. Crossref

8. Rubešová K, Jakeš V, Hlásek T. Bi-Sr-Co-O thermos-electrics prepared by sol-gel methods with modified gel decomposition. Journal of Physics and Chemistry of Solids. 2012; 73(3):448–53. Crossref

9. Wang W, Chen Q, Cui Q. Improvement in structure and superconductivity of YBa2Cu3O6+ δ ceramics superconductors by optimizing sintering processing. Physica C: Superconductivity and its Applications. 2015; 511:1–3.

10. Wang X, Lu M, Qiu L. Graphene/titanium carbide composites prepared by sol–gel infiltration and spark plasma sintering. Ceramics International, 2016; 42(1):122–31. Crossref

11. Abbasi Z, Bahrololoum M, Bagheri, R. Characterization of the bioactive and mechanical behavior of dental ceramic/sol–gel derived bioactive glass mixtures. Journal of the Mechanical Behavior of Biomedical Materials. 2016; 54:115–22. Crossref. PMid:26454135

12. Mackenzie J, Ulrich D. Ultrastructure Processing of Advanced Ceramics. New York: Wiley; 1988.

13. Gua H, Dongb C, Chena P, Kuanga A, Lic X. Growth of layered perovskite Bi4Ti3O12 thin films by sol–gel proces. Journal of Crystal Growth. 1998; 186(3):403–8. Crossref

14. Veber A, Kunej S, Suvorov D. Synthesis and microstructural characterization of Bi12SiO20 (BSO) thin films produced by the sol–gel process. Ceramics International. 2010; 36(1):245–50. Crossref

15. Maniscalco S, Caligari Conti M, Cassar J, Grima C, Karl A, Wismayer PS, Mallia B, Buhagiar J. Low temperature carburised austenitic stainless steel for metal-on-metal tribological contact. Thin Solid Films. 2016; 620:103–13. Crossref

16. Chang K, Chung SC, Lai S. The Electrochemical Behavior of Thermally Oxidized CrN Coatings Deposited on Steel by Cathodic Arc Plasma Deposition. Applied Surface Science. 2004; 236(1):406–15. Crossref

17. Altun H, Sen S. The effect of DC magnetron sputtering AlN coatings on the corrosion behavior of magnesium alloys. Surface and Coatings Technology. 2005; 197(2):193–200. Crossref

18. Moreno C, Hernández S, Santana J. Characterization of Water Uptake by Organic Coatings Used for the Corrosion Protection of Steel as Determined from Capacitance Measurements. International Journal of Electrochemical Science. 2012; 7:8444–57.

19. Yoo Y, Le D, Kim S. Corrosion behavior of TiN, TiAlN, TiAlSiN thin films deposited on tool steel in the 3.5 wt. % NaCl solution. Thin Solid Films. 2008; 516(11):3544–8. Crossref

20. Xin Z, Lei M, Jian-gang W, Hui-min Z. Investigation on ultrathin titanium oxide films synthesized by surface sol-gel method. Optik - International Journal for Light and Electron Optics. 2016; 127(5):2780–3.